

**IMPROVING MULTIFERROIC EFFICIENCY IN PARTICULATE MULTIFERROIC COMPOSITE MATERIALS OF COBALT FERRITE AND SAMARIUM-DOPED BARIUM TITANATE**

**Showket Ahmad Bhat<sup>\*</sup>, Ab Mateen Tantray and M. Ikram**

Department. of Physics, NIT Srinagar, J&K 190006, India

\*showketbht7@gmail.com

**ABSTRACT**

*Using a variety of characterisation methods, we examined the multiferroic behavior of composite materials made up of  $(1-x)$  Ba<sub>0.5</sub>Sm<sub>0.5</sub>TiO<sub>3</sub> (SmBT) and  $x$ Co<sub>0.5</sub>Sm<sub>0.5</sub>Fe<sub>2</sub>O<sub>3</sub> (SmCF) in this work. A 0–3 particulate connection technique was used to produce the composites, allowing for straightforward fabrication without the need for sophisticated machinery. To investigate the composites' local structure, Raman spectroscopy was used. The intended crystal structure was confirmed by the Raman spectra, which showed distinctive optical modes matching to the tetragonal P4mm crystal symmetry. The spectra also showed lattice disorder brought on by the addition of SmCF and metal-oxygen vibrations.*

*The ferrimagnetic behavior of the composites was investigated by magnetic experiments. Within domains, exchange interactions between spins with various orientations were suggested by saturated M-H loops. Saturation magnetization and magnetic moments rose with increasing SmCF content in the composites, suggesting greater exchange interactions. Every sample had multi-domain structures, according to the domain structure analysis.*

*Keywords: Multiferroic composites, Raman spectroscopy, X-ray photoelectron spectroscopy, spectroscopic characterization, crystal structure.*

**INTRODUCTION**

It is often known that materials science is one of the major factors impacting economic growth and development. Since the industrial revolution in silicon in the 1950s, research and developments in solid-state science and materials have had a significant influence on and revolutionized our civilization. In materials science, a material becomes multifunctional when it possesses numerous beneficial characteristics. Multiferroics are materials having multiple applications that combine two or more fundamental ferroic states, like ferroelectricity, ferromagnetism, ferroelasticity, and ferrotoroidicity [1,2]. Science has focused a great deal of interest on multiferroic materials that show the presence of at least ferroelectric and ferro/ferrimagnetic orders. In reaction to an external field, ferroic materials frequently alter their internal alignment. External magnetic and electrical forces may regulate the alignment of electrical dipoles and spins in polarizable materials.

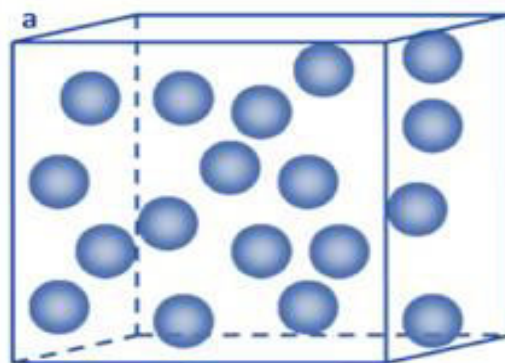


**Fig.1.1** Diagrammatic representation of a bulk composite with 0-3 particulate connection scheme.

A commonly used method to enhance the ferroic properties of multiferroic composites involves maximizing strain transfer between the magnetic and electric phases. This is achieved by selecting a ferroelectric phase with low

leakage currents and a magnetic phase with high magnetic moment and magnetostriction. Such a combination can lead to an improved magnetoelectric (ME) response at the boundary interface, potentially enhancing the overall ME performance of the composite material. The ME response of multiferroic composites is measured by the ratio of polarization (P) induced by an applied magnetic field (H). This phenomenon is mathematically described as the direct ME effect [3-5].

$$\alpha_H = \frac{\partial P}{\partial H} \cong \varepsilon_o \varepsilon_r \left( \frac{\partial E}{\partial H} \right) \quad 1$$

$$As, \quad P = \varepsilon_o \chi E = \varepsilon_o (\varepsilon_r - 1) E = \varepsilon_o \varepsilon_r E \quad for \varepsilon_r \gg 1 \quad 2$$

where  $\varepsilon_o$  and  $\varepsilon_r$  are, respectively, the relative permittivity of the medium and the dielectric permittivity of the object. Since  $E = V/t$ , where V is the voltage and t are the thickness, the following relationship for the magnetically generated magnetoelectric effect is discovered

$$\alpha_H = \frac{\partial P}{\partial H} \cong \varepsilon_o \varepsilon_r \left( \frac{\partial E}{\partial H} \right) = \frac{\varepsilon_o \varepsilon_r}{t} \left( \frac{\partial V}{\partial H} \right) = \alpha_H^V \varepsilon_o \varepsilon_r \quad 3$$

where  $\alpha_H^V$  is the magnetoelectric coefficient, which is defined as:

$$\alpha_H^V = \frac{\partial E}{\partial H} = \frac{1}{t} \left( \frac{\partial V}{\partial H} \right) \quad 4$$

The primary parameter utilized in assessing experimental data and developing different multiferroics-based applications is the voltage magneto-electric coefficient ( $\alpha$ ).

There has been a lot of research done on the materials Ba(Ti, Sn)O<sub>3</sub>–(Ba, Ca)TiO<sub>3</sub> (whose piezoelectric coefficient is  $d_{33} \sim 550$  pC N<sup>-1</sup>) and Ba(Ti, Hf)O<sub>3</sub>–(Ba, Ca)TiO<sub>3</sub> (whose piezoelectric coefficient is  $d_{33} \sim 550$  pC N<sup>-1</sup>). These materials' 0.5BZT-0.5BCT or BCTZ composition, which corresponds with the morphotropic phase boundary (MPB) composition, is responsible for their higher piezoelectric sensitivity. As with lead zirconate titanate (PZT), this alignment results in a decrease of free energy anisotropy. With a notable piezoelectric coefficient, Ba<sub>0.85</sub>Ca<sub>0.15</sub>Ti<sub>0.9</sub>Zr<sub>0.1</sub>O<sub>3</sub>, or 0.5BZT-0.5BCT, has shown promise as an alternative to conventional lead-based piezoelectric materials. Strong magnetoelectric (ME) coupling effect is best achieved using ferrites that show high magnetostriction and ferroelectric materials based on the ABO<sub>3</sub> structure, which show a significant piezoelectric coefficient. Widespread documentation of the piezoelectric effect in BCT-based ABO<sub>3</sub> materials highlights their potential in the creation of multiferroic composites devoid of lead that can generate a sizable ME response. Compared to BaTiO<sub>3</sub>, which has a Curie temperature of about 120 °C, BCT has a Curie temperature of about 90 ± 10 °C. The ferroelectric crystal structure undergoes symmetry transformations from rhombohedral to orthorhombic and finally tetragonal as the BCT concentration rises. Cobalt ferrite (CoFe<sub>2</sub>O<sub>4</sub>) is widely recognized for its remarkable magnetic characteristics, which include having a high Curie temperature and the highest magnetostriction coefficient ( $k \sim -110 \times 10^{-6}$ ) of any ferrite family. Because of this, investigating composite structures that combine BCT and CoFe<sub>2</sub>O<sub>4</sub> (CFO) is a worthwhile line of inquiry. Scientists have created nanocomposites like xBa<sub>0.8</sub>Ca<sub>0.2</sub>TiO<sub>3</sub>-(1-x)Ni<sub>0.2</sub>Cu<sub>0.3</sub>Zn<sub>0.5</sub>Fe<sub>2</sub>O<sub>4</sub> by adjusting the value of x. They discovered that when x = 0.3, the greatest magnetoelectric coefficient of 280 mV/cm Oe was recorded.

### Raman Spectroscopy

Using a T64000 Horiba-Jobin Yvon triple-monochromator spectrometer with a confocal microscope and a liquid N<sub>2</sub> cooled charge coupled device, Raman spectra were obtained (CCD). Using an argon ion laser at 514.5 nm, the scattering was stimulated. In order to prevent sample heating, the laser's spot size was 1 $\mu$ m<sup>2</sup> utilizing a 100X objective lens and its power was fixed at 1.0mW. It is highly sensitive spectroscopic technique to probe the local

structure of atoms and materials. In a cubic perovskite structure optical-vibration are triply degenerate  $F_{1u}$  and  $F_{2u}$  modes. As there are no asymmetries in cubic phase therefore  $F_{1u}$  mode is Raman inactive. Whereas  $F_{1u}$  and  $F_{2u}$  modes splits into A, E and B, E modes respectively in tetragonal phase as  $4E+3A+B$ . The long range of electrostatic forces acting on these modes as they exist in transverse and longitudinal modes[5-7]. In figure 2 the Raman spectra of SmBT-SmCF(0.02), SmBT-SmCF(0.04) and SmBT-SmCF(0.06) optical modes are visible around at 190, 239, 308, 721  $\text{cm}^{-1}$  and validate the symmetry of the tetragonal  $P4mm$  crystal [8]. The non-symmetric metal-oxygen vibration of phonons and transverse non-symmetry vibration  $A_T$  are correlated at 180  $\text{cm}^{-1}$  the incorporation SmCF in the SmBT produce the lattice disorder which shows the spectrum between 200-275  $\text{cm}^{-1}$  [9].  $E_L$  and  $E_T$  modes are present at 306  $\text{cm}^{-1}$  and at 713  $\text{cm}^{-1}$  symmetric stretching  $A_L$  modes are present that shows resemblance to the tetragonal ferroelectric phase of  $\text{BaTiO}_3$ . At 512  $\text{cm}^{-1}$  a transverse  $A_L$  mode of  $\text{TiO}_6$  present. The peak's existence at 680  $\text{cm}^{-1}$  ensures the composite's validity. The metal-oxygen migration at the tetrahedral sites in  $\text{CoFe}_2\text{O}_4$  is shown by the origin of the frequency peak at 678  $\text{cm}^{-1}$  [10].

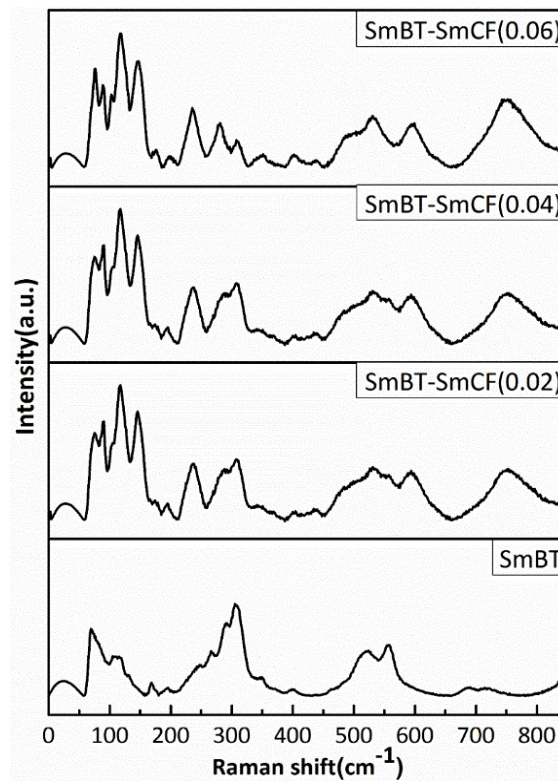
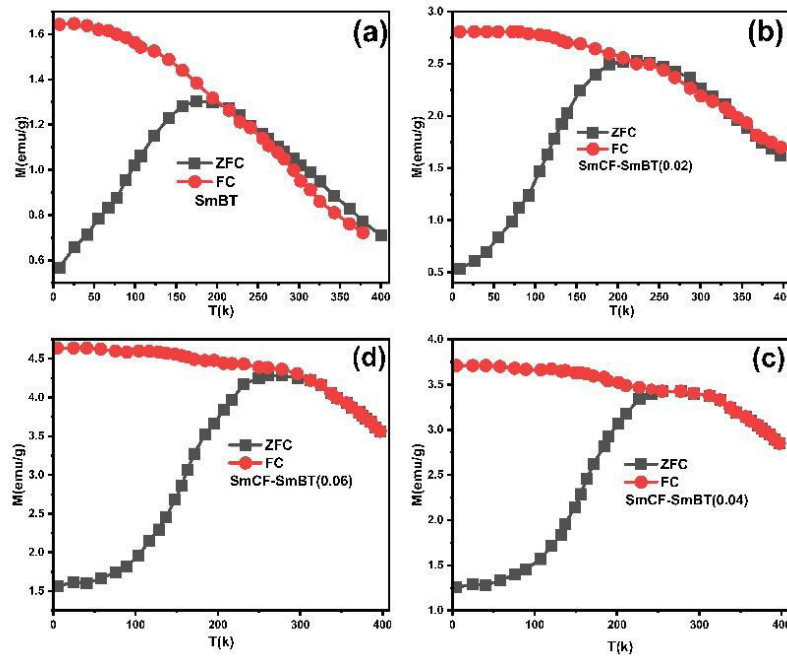


**Figure 1:** Raman spectra of composites  $(1-x)\text{Ba}_{0.5}\text{Sm}_{0.5}\text{TiO}_3-x\text{Co}_{0.5}\text{Sm}_{0.5}\text{Fe}_2\text{O}_3$  ( $x=0.0, 0.02, 0.04, 0.06$ ).

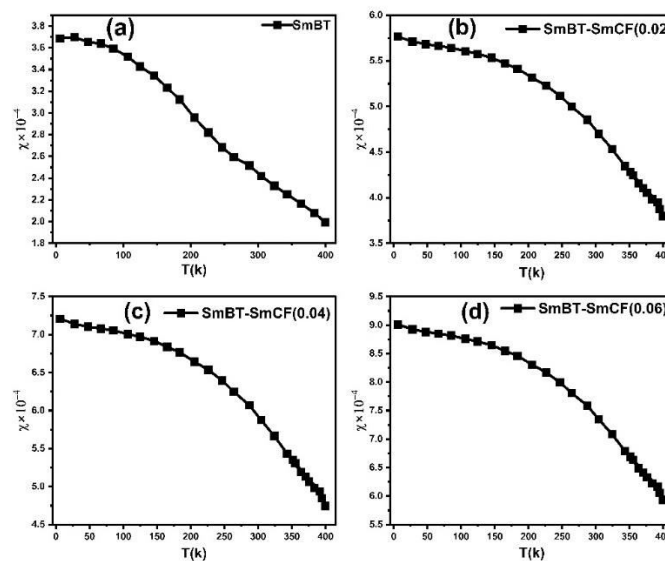
### Temperature Dependent Magnetic Study

Figure 3 displays the magnetization's temperature dependence within the range of 0-400 K for the composites. In the absence of a magnetic field, during the process of zero field cooling (ZFC), the spins within the composites become immobilized and oriented in various directions. The cessation of the magnetic field results in a reduction of magnetization at lower temperatures[11-13]. Upon subjecting the system to a magnetic field of 4 kOe, specifically through the process of field cooling (FC), an augmentation in magnetization is detected, in accordance with the existing literature [14]. The phenomenon of magnetization in relation to temperature can be elucidated by considering the spontaneous magnetization of the two sub-lattices in the SmCF phase. These sub-lattices possess distinct magnetization values,  $M_A$  and  $M_B$ , and are oriented in an anti-parallel manner. The magnetization resulting from the difference between  $M_A$  and  $M_B$ . The rate of decrease in magnetization ( $M_B$ ) of one sublattice is slower than that of another sublattice with magnetization ( $M_B$ ) as the temperature decreases. This leads to an augmentation in the overall magnetization. At elevated temperatures, the thermal agitation of spins

disrupts the magnetic couplings, leading to a reduction in magnetization. Moreover, it has been observed that composites exhibit an increase in magnetization as the SmCF phase is raised during the process of field cooling. This phenomenon is attributed to the increase in the alignment of spins in the direction of the magnetic field. The magnetic susceptibility exhibited a similar pattern during the process of field cooling, as depicted in Figure 4, to that of magnetization. An observed decrease in the Curie temperature ( $T_C$ ) from 0.06 to 0.02 can be attributed to the weakening of various magnetic linkages that contribute to magnetism, caused by the presence of the non-magnetic SmBT phase.



**Figure 3:** Field cooling and zero field cooling of  $(1-x)Ba_{0.5}Sm_{0.5}TiO_3-xCo_{0.5}Sm_{0.5}Fe_2O_3$  ( $x=0.0,0.02,0.04,0.06$ ).



**Figure 4:** variation of magnetic susceptibility with temperature for particulate of  $(1-x)Ba_{0.5}Sm_{0.5}TiO_3-xCo_{0.5}Sm_{0.5}Fe_2O_3$  ( $x=0.0,0.02,0.04,0.06$ ).



**Magnetoelectric Coupling**

In this work, we looked at the magnetoelectric connection between the magnetic SmCF phase and the ferroelectric SmBT phase. We used the dynamic technique, which includes applying both an AC magnetic field and a static DC magnetic field. The AC magnetic field ( $H_{AC}$ ) had a frequency of 1 kHz and a constant amplitude of 1Oe, but the DC magnetic field ( $H_{DC}$ ) varied in field intensity from 0 to 4 kOe. In order to start the experiment, we electrically polarized every composite, creating a finite electric polarisation. After that, the electrically polarized composites were arranged parallel to the magnetic field's axis. This experimental set-up was used to ascertain the degree of interaction between the ferroelectric SmBT and magnetic SmCF phases. Changes in the ferroelectric characteristics were caused by the interaction of the magnetic field-induced strain in the magnetic phase (due to magnetostriction) and the ferroelectric phase. We were able to assess this magnetoelectric coupling effect's size using the dynamic technique [15-18]. Utilizing the magnetoelectric effect, the application of a magnetic field induces a voltage ( $\delta V$ ) in the material under study. This induced voltage was then measured and detected using a lock-in amplifier. The ME coefficient ( $\alpha$ ) was determined using relation 8 [19].

$$\alpha = \frac{\delta V}{t \times H_{AC}} \quad 16$$

where  $t$  is the particulate composites thickness, measured in terms of pellet thickness. And  $\delta V$  is given by

$$\delta V = V_{(H_{DC}=H)} + V_{(H_{DC}=0)}.$$

According to prior study, the magneto-strictive strain ( $\lambda$ ) is reliant on the piezo-magnetic coefficient ( $q$ ), which in turn affects the coupling coefficient ( $\alpha$ ) [20]. Mathematically, the coefficient ( $q$ ) is defined as the derivative of  $\lambda$  with respect to the applied magnetic field ( $q = d\lambda/dH$ ). In the present investigation, a rise in the magnetic field is accompanied by a rise in the magneto-strictive strain ( $\lambda$ ). For a certain value of the applied magnetic field, a maximum is seen. Beyond this maximum an  $\alpha$  is shown to go down, and at high magnetic fields, a little change is seen. The decline in  $\alpha$  is attributed to the magnetic field is applied parallel to the polarisation, i.e.,  $H$  and  $E$  are parallel to one another, supports the observed behavior of  $\alpha$ . The coupling coefficients are, however, quite small when the  $P$  and  $H$  are perpendicular to one another [21,22]. The primary working principle behind this technique is the creation of strain in the ferromagnetic SmCF phase as a result of the applied magnetic field. After that, by the motion of domain walls, this strain is transmitted to the ferroelectric SmBT phase. The SmBT phase as a consequence produces an induced magnetoelectric (ME) voltage. The increased elastic interaction between the SmBT and SmCF phases is primarily responsible for the rise in  $\alpha$  [23]. All composites of the coupling coefficient in a given field exhibit a peak, which is followed by partial saturation. The  $M$ -  $H$  hysteresis loops provide more evidence that the peak is located near the saturation field (1.5 kOe). Peak values are produced at the saturation field, when the most strain is transmitted from the magnetic SmCF phase to the ferroelectric SmBT phase [24]. Given the larger concentration of the magnetic SmCF phase, it is not surprising that SmBT-XSmCF ( $X=0.06$ ) has a maximum in, followed by 0.04 and 0.02. Because 0.06 has larger grains and high porosity, maximal strain transmission across grain boundaries is possible, and this results in the higher value as seen in figure 11. This study's detection of a high coupling value in comparison to previous rare-earth doped particle composites [24-26] is an important finding.

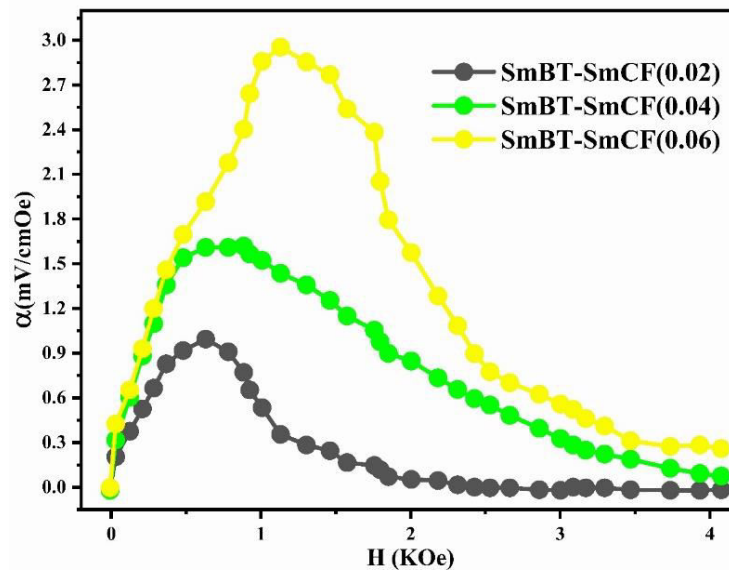


**Figure 5:** Plots illustrating the fluctuation of the coupling coefficient ( $\alpha$ ) as a function of the magnetic field ( $H$ ) for composites SmBT-XSmCF ( $X=0.02,0.04,0.06$ ).

## CONCLUSION

To sum up, the multiferroic characteristics of composites made from the  $(1-x)\text{Ba}0.5\text{Sm}0.5\text{TiO}3-x\text{Co}0.5\text{Sm}0.5\text{Fe}2\text{O}3$  framework were the main focus of our investigation. Several connection strategies, such as the 0–3 particulate composite, which is renowned for its ease of manufacturing, were successfully used to build the composites. We were able to obtain important insights into the structural and magnetic properties of these composites by using a variety of characterisation techniques.

The tetragonal  $P4mm$  crystal structure was confirmed by using Raman spectroscopy to determine the optical vibration modes and phonons related to the crystal symmetry. According to magnetic studies, the composites showed ferrimagnetic behavior, with increased concentrations of the magnetic phase (SmCF) corresponding to increases in saturation magnetization and magnetic moments. The critical temperature ( $T_c$ ) and dielectric constant ( $\epsilon_r$ ) increased with the introduction of the SmCF phase because of internal tensions and electron hopping processes. The composites exhibited dielectric loss ( $\tan\delta$ ) peaks in the vicinity of the Curie temperatures, suggesting that they could find use in multiferroic applications. Furthermore, domain analysis revealed a multi-domain architecture that was complicated and was attributed to the ferroelectric SmBT phase-induced pinning effects.

## ACKNOWLEDGEMENT

The Central Research Facility Centre (CRFC) of the National Institute of Technology (NIT), Srinagar is highly regarded for its provision of instrumentation facilities. The authors further expresses gratitude for the financial support provided by the Ministry of Human Resources Development (MHRD).

## Declaration of Competing Interest

The authors state that they have no financial conflicts of interest or personal ties that could have influenced the research presented in this study.

## Author Contributions:

**Showket Ahmad Bhat:** Conceptualization, Methodology, Experimentation, Validation, Formal Analysis and Writing Original Draft

**Ab Mateen Tantray:** Experimentation, Validation, Formal Analysis and Writing Original Draft

**Prof. M Ikram:** Conceptualization, Resource, Visualization, Validation, Supervision, and Revision

**Data Availability:** All data generated or analyzed during this study are included in this article.

#### REFERENCES

- [1] M. M. Vopson, "Fundamentals of Multiferroic Materials and Their Possible Applications," pp. 1–28, 2014, doi: 10.1080/10408436.2014.992584.
- [2] C.-W. Nan, M. I. Bichurin, S. Dong, D. Viehland, and G. Srinivasan, "Multiferroic magnetoelectric composites: Historical perspective, status, and future directions," *J. Appl. Phys.*, vol. 103, no. 3, Feb. 2008, doi: 10.1063/1.2836410.
- [3] S. Q. Ren, L. Q. Weng, S. H. Song, F. Li, J. G. Wan, and M. Zeng, "BaTiO<sub>3</sub>/CoFe<sub>2</sub>O<sub>4</sub> particulate composites with large high frequency magnetoelectric response," *J. Mater. Sci.*, vol. 40, no. 16, pp. 4375–4378, 2005, doi: 10.1007/s10853-005-1057-1.
- [4] A. S. Kumar, C. S. C. Lekha, S. Vivek, K. Nandakumar, M. R. Anantharaman, and S. S. Nair, "Effect of CoFe<sub>2</sub>O<sub>4</sub> weight fraction on multiferroic and magnetoelectric properties of (1 – x)Ba<sub>0.85</sub>Ca<sub>0.15</sub>Zr<sub>0.1</sub>Ti<sub>0.9</sub>O<sub>3</sub> – xCoFe<sub>2</sub>O<sub>4</sub> particulate composites," *J. Mater. Sci. Mater. Electron.*, vol. 30, no. 9, pp. 8239–8248, 2019, doi: 10.1007/s10854-019-01140-3.
- [5] K. Kaur, M. Singh, J. Singh, and S. Kumar, "Multiferroic and magnetodielectric properties of (1-x)KNN-xCMgFO ceramic-based composites," *J. Asian Ceram. Soc.*, vol. 8, no. 4, pp. 1027–1035, 2020, doi: 10.1080/21870764.2020.1803534.
- [6] Z. Zhao et al., "Grain-size effects on the ferroelectric behavior of dense nanocrystalline BaTiO<sub>3</sub> ceramics," *Phys. Rev. B - Condens. Matter Mater. Phys.*, vol. 70, no. 2, pp. 1–8, 2004, doi: 10.1103/PhysRevB.70.024107.
- [7] S. Indla, A. Chelvane, A. Lodh, and D. Das, "Enhancement in magnetostrictive properties of cobalt ferrite by magnetic field assisted compaction technique," *J. Alloys Compd.*, vol. 779, pp. 886–891, 2019, doi: 10.1016/j.jallcom.2018.11.313.
- [8] P. Pahuja, R. K. Kotnala, and R. P. Tandon, "Effect of rare earth substitution on properties of barium strontium titanate ceramic and its multiferroic composite with nickel cobalt ferrite," *J. Alloys Compd.*, vol. 617, pp. 140–148, 2014, doi: 10.1016/j.jallcom.2014.07.204.
- [9] G. Lawes and G. Srinivasan, "Introduction to magnetoelectric coupling and multiferroic films," *J. Phys. D. Appl. Phys.*, vol. 44, no. 24, 2011, doi: 10.1088/0022-3727/44/24/243001.
- [10] J. Ma, J. Hu, Z. Li, and C. W. Nan, "Recent progress in multiferroic magnetoelectric composites: From bulk to thin films," *Adv. Mater.*, vol. 23, no. 9, pp. 1062–1087, 2011, doi: 10.1002/adma.201003636.
- [11] W. Liu and X. Ren, "Large piezoelectric effect in Pb-free ceramics," *Phys. Rev. Lett.*, vol. 103, no. 25, pp. 1–4, 2009, doi: 10.1103/PhysRevLett.103.257602.
- [12] S. Kumar, G. A. Kaur, A. Saha, and M. Shandilya, "Influence of Ga<sub>2</sub>O<sub>3</sub> on structural and morphological properties of lead-free BCT at low temperature," *AIP Conf. Proc.*, vol. 2357, no. May, 2022, doi: 10.1063/5.0080987.
- [13] M. Zakhozheva, L. A. Schmitt, M. Acosta, W. Jo, J. Rödel, and H. J. Kleebe, "In situ electric field induced domain evolution in Ba(Zr<sub>0.2</sub>Ti<sub>0.8</sub>)O<sub>3</sub>-0.3(Ba<sub>0.7</sub>Ca<sub>0.3</sub>)TiO<sub>3</sub> ferroelectrics," *Appl. Phys. Lett.*, vol. 105, no. 11, pp. 2–6, 2014, doi: 10.1063/1.4896048.

- [14] P. W. Rehrig, S. E. Park, S. Trolier-McKinstry, G. L. Messing, B. Jones, and T. R. Shrout, "Piezoelectric properties of zirconium-doped barium titanate single crystals grown by templated grain growth," *J. Appl. Phys.*, vol. 86, no. 3, pp. 1657–1661, 1999, doi: 10.1063/1.370943.
- [15] K. Sadhana et al., "Magnetic field induced polarization and magnetoelectric effect of Ba<sub>0.8</sub>Ca<sub>0.2</sub>TiO<sub>3</sub>-Ni<sub>0.2</sub>Cu<sub>0.3</sub>Zn<sub>0.5</sub>Fe<sub>2</sub>O<sub>4</sub> nanomultiferroic," *J. Appl. Phys.*, vol. 113, no. 17, pp. 8–11, 2013, doi: 10.1063/1.4795820.
- [16] L. V. Leonel, A. Righi, W. N. Mussel, J. B. Silva, and N. D. S. Mohallem, "Structural characterization of barium titanate-cobalt ferrite composite powders," *Ceram. Int.*, vol. 37, no. 4, pp. 1259–1264, 2011, doi: 10.1016/j.ceramint.2011.01.017.
- [17] M. Naveed-Ul-Haq et al., "A new (Ba, Ca) (Ti, Zr)O<sub>3</sub> based multiferroic composite with large magnetoelectric effect," *Sci. Rep.*, vol. 6, no. January, pp. 1–10, 2016, doi: 10.1038/srep32164.
- [18] R. Sharma, P. Pahuja, and R. P. Tandon, "Structural, dielectric, ferromagnetic, ferroelectric and ac conductivity studies of the BaTiO<sub>3</sub>-CoFe<sub>1.8</sub>Zn<sub>0.2</sub>O<sub>4</sub> multiferroic particulate composites," *Ceram. Int.*, vol. 40, no. 7 PART A, pp. 9027–9036, 2014, doi: 10.1016/j.ceramint.2014.01.115.
- [19] Kavita Verma, M. K. Shamim, S. Kumar, and S. Sharma, "Role of ferrite phase on the structural, ferroelectric and magnetic properties of (1-x) BCT-x CZFO composites," *Mater. Chem. Phys.*, vol. 255, no. November 2019, p. 123284, 2020, doi: 10.1016/j.matchemphys.2020.123284.
- [20] S. Shankar, O. P. Thakur, and M. Jayasimhadri, "Conductivity behavior and impedance studies in BaTiO<sub>3</sub>-CoFe<sub>2</sub>O<sub>4</sub> magnetoelectric composites," *Mater. Chem. Phys.*, vol. 234, pp. 110–121, Aug. 2019, doi: 10.1016/j.matchemphys.2019.05.095.
- [21] Z. Yao et al., "Structure and dielectric behavior of Nd-doped BaTiO<sub>3</sub> perovskites," *Mater. Chem. Phys.*, vol. 109, no. 2–3, pp. 475–481, Jun. 2008, doi: 10.1016/j.matchemphys.2007.12.019.
- [22] I. Coondoo, N. Panwar, H. Amor, V. E. Ramana, and A. Kholkin, "I. Coondoo, N. Panwar, H. Amor, V. E. Ramana, and A. Kholkin, "Indrani Coondoo, Neeraj Panwar, Harvey Amor in, Venkata Eszilla Ramana," vol. 3135, pp. 3127–3135, 2015, doi: 10.1111/jace.13713.
- [23] W. B. White and B. A. D. Anolis, "Interpretation of the vibrational spectra of spinels," vol. 25, no. 1964, 1967, doi: [https://doi.org/10.1016/0584-8539\(67\)80023-0](https://doi.org/10.1016/0584-8539(67)80023-0).
- [24] Y. Shen et al., "The enhanced magnetodielectric interaction of (1 - X)BaTiO<sub>3</sub>-xCoFe<sub>2</sub>O<sub>4</sub> multiferroic composites," *J. Mater. Chem. C*, vol. 2, no. 14, pp. 2545–2551, 2014, doi: 10.1039/c4tc00008k.
- [25] D. Basandrai, "Magnetic properties of bismuth substituted strontium ferrite nanoparticles," *Eur. J. Mol. Clin. Med.*, vol. 7, no. 7, pp. 3432–3437, 2020.
- [26] E. C. Devi and S. D. Singh, "Understanding low-temperature magnetization curves with law of approach to saturation in Co<sub>0.5</sub>Zn<sub>0.5</sub>Fe<sub>2</sub>O<sub>4</sub>," *J. Mater. Sci. Mater. Electron.*, vol. 33, no. 29, pp. 22751–22758, 2022, doi: 10.1007/s10854-022-09042-7.